Installation and performance of the 3rd Veto plane at the SND@LHC detector

The SND@LHC collaboration

E-mail: giulia.paggi@cern.ch

ABSTRACT: During 2022/2023 the optimal inefficiency of the Veto system of the SND@LHC detector was measured to be $(7.8 \pm 2.8) \times 10^{-8}$. To reduce this inefficiency, a third Veto plane was installed during the 2023-2024 Year End Technical Stop. In addition, the Veto system was lowered to cover the target fully, thereby increasing acceptance. This paper describes how the inefficiency of the Veto system was reduced from $(7.8 \pm 2.8) \times 10^{-8}$ with an acceptance of about 64% of the target area in 2022–2023 to $(4.9 \pm 1.9) \times 10^{-9}$ on the full area in 2024.

Contents

1 Introduction

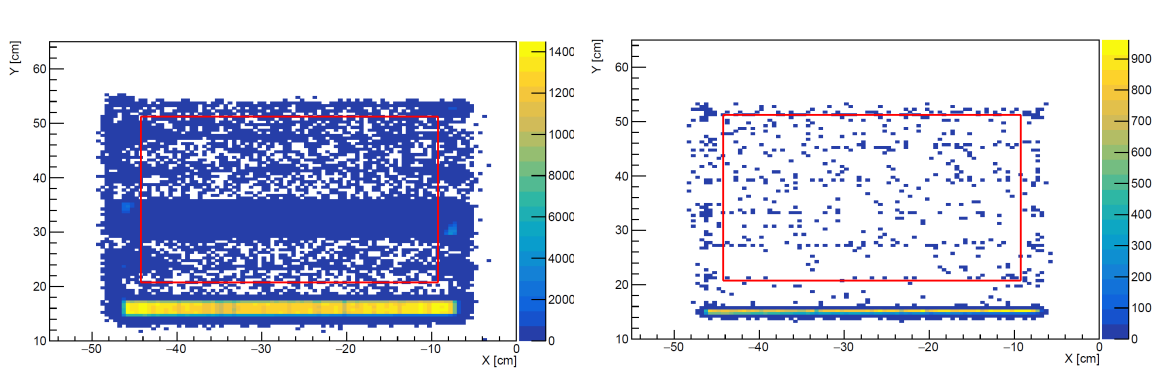The Scattering and Neutrino Detector at the LHC (SND@LHC) is a compact, stand-alone experiment to perform measurements with neutrinos produced at the LHC in the pseudo-rapidity region of $7.2 < \eta < 8.4$ [1]. The experiment is located 480 m downstream of the ATLAS interaction point, in the unused TI18 tunnel. It comprises a Veto system to identify incoming charged particles (mostly muons), a target region where neutrinos interact, a hadronic calorimeter (HCAL) and a muon identification system. The target region consists of bricks of emulsion cloud chambers. The emulsion cloud chambers bricks are interleaved with scintillating fibre (SciFi) tracker layers, which allow the identification of candidates for neutrino interactions. The Veto, HCAL and Muon systems use scintillating bars with different geometries: 6 cm bars in the Veto and upstream part of the HCAL, to achieve a high detection efficiency and energy resolution respectively, and 1 cm bars in the downstream part, to effectively isolate and measure the position and angle of crossing muons. In 2022, the Veto system had two Veto planes. One Veto plane consists of 7 bars and each bar is read by 16 silicon photomultipliers (SiPMs), 8 on each end (see figure 1).

Figure 1. Layout of the SND@LHC detector.

Using data collected in 2022, we reported the observation of neutrino interactions from ν_μs originating at the LHC IP1 [2]. To obtain this result it was necessary to achieve a pure set of neutrino signals over background by applying selection cuts with a strong rejection power.

In 2022-2023 the inefficiency of the Veto system was dependent on the data taking condition but the optimal value measured to be $(7.8 \pm 2.8) \times 10^{-8}$ on a fiducial area of 35×35 cm^2, corresponding to a target coverage of $\sim 64\%$. To obtain the required rejection power, the first two SciFi planes were added to the Veto system which significantly reduced the fiducial volume. The background from muons was now negligible, but this fiducial volume cut rejects 92.4% of the neutrino charged current interactions. This is because the neutrino density is higher in the bottom part of the detector (see figure 2).

Figure 2. The extrapolated position of the reconstructed Scifi track at Veto plane 1 (left) and Veto plane 2 (right). The red square encloses the fiducial area, which was used for the observation of neutrino interactions [2]. The density of muon tracks at the bottom is higher due to the convolution of the veto geometrical acceptance and the muon flux distribution measured in the detector [3].

To improve the efficiency of the Veto system, a third Veto station with vertical bars was installed during the Year End Technical Stop of 2023–2024 (see figure 3). Moreover, the whole Veto system was lowered by ≈ 27 cm to provide full coverage of the target by all stations.
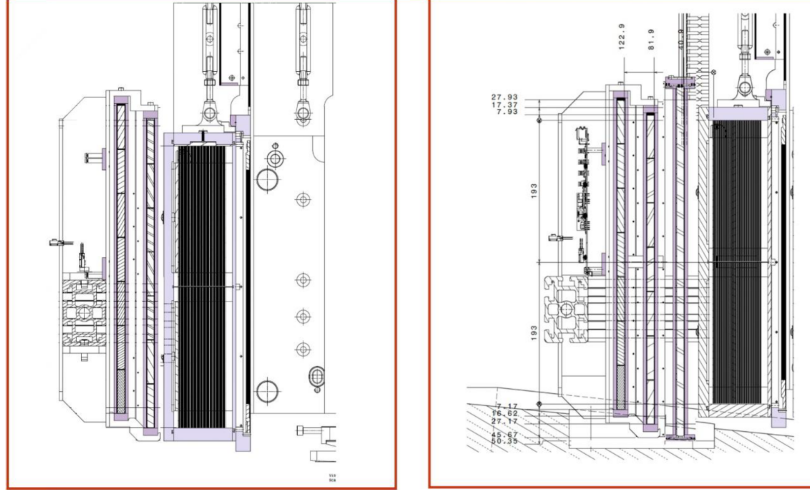
In this paper, we report on the construction of the Veto 3 plane, its performance during commissioning with cosmic rays, its installation in TI18, the measured system inefficiency results, and provide an estimate of the expected increase in the number of observed neutrino interactions.

2 Design and construction

The Veto 3 module, made of scintillating bars read out by SiPMs, uses the same technology as Veto 1 and 2 [1].

While Veto 1 and 2 have horizontally disposed bars, the Veto 3 bars are aligned vertically (see figure 4, top). The Veto 3 bars are 46 cm long, extending by 2 cm above and below the Veto 1 and 2 range (see figure 3).

The Veto 3 bars are read out at the top edge by 56 Hamamatsu Photonics MPPC S14160-6050HS SiPMs (6×6 mm^2, 50 μm pitch) [4] hosted on a printed circuit board (PCB) and subdivided in seven equally spaced bunches, which are carefully aligned to be centered between bar edges, so that each bar is uniquely read out by 8 SiPMs (see figure 4, bottom).

Figure 3. Current Veto system layout with two planes with horizontal bars (left). The upgraded Veto system with a third plane with vertical bars (right).

To ensure optimal readout the bar edges are placed in close contact with the SiPMs without using optical gel, while the other side is carefully closed with flat aluminized mylar pieces to act as efficient mirrors.

As for Veto 1 and 2, the SiPMs signals are routed to the front-end PCB, which is mounted on the Veto 3 module and hosts two TOFPET ASICs [5], each viewing 28 SiPMs.

The vertical disposition of bars in Veto 3 minimises the probability that the readout dead time coincides with the passage of a second muon through the same bar. Although Veto 1 and Veto 2 are staggered, there remains a possibility that two muons could traverse the overlapping region. If the time interval between the two particles is sufficiently short, the signal from the second muon may be lost due to the time required to process the signal from the first. The vertical bars in Veto 3 provide an additional vertical segmentation, thereby reducing the overlapping region among the three bars. This minimizes the probability of two muons hitting the detector so close in space and time that no signal is left in any of the Veto planes.
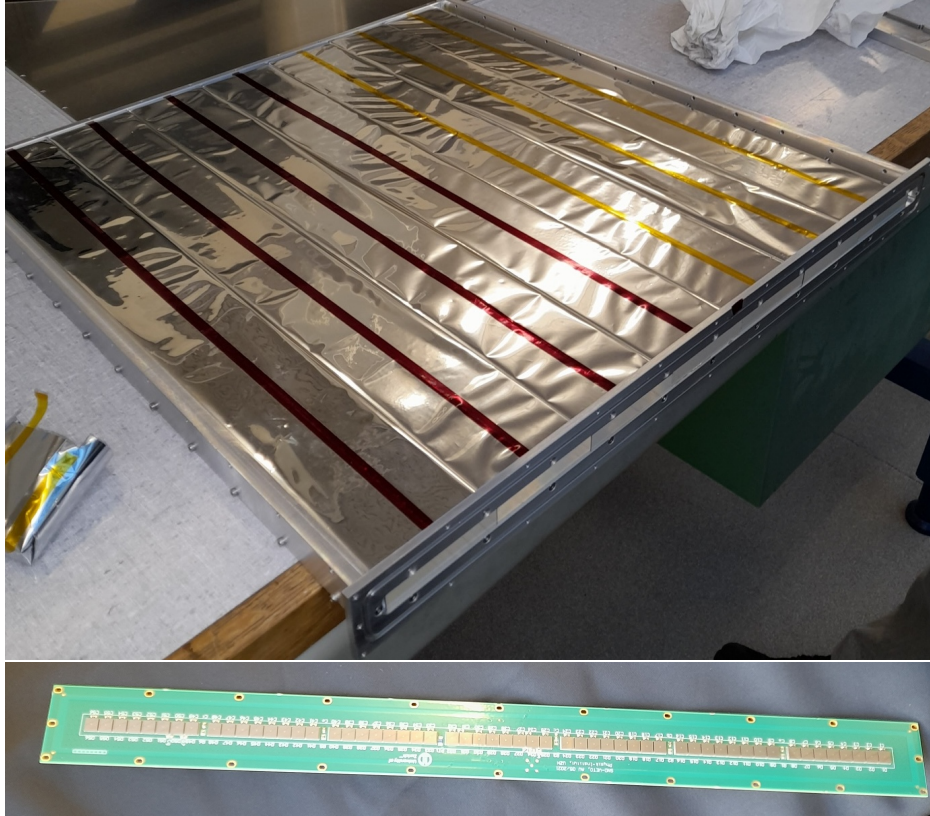
The completed Veto 3 module was tested for electrical and light tightness. The SiPM dark count rate was measured to set a suitably low noise level.

3 Performance with cosmic rays

The Veto 3 module was first tested with a dedicated laboratory setup to check that all channels were efficient and to look for systematic asymmetries in the efficiency along the bars, between the bar end close to the SiPMs and the opposite reflective end.

The setup that was used for this test consisted of the Veto 3 module and a SND@LHC DownStream (DS) chamber.

The DS chamber consists of $82.5 \times 1 \times 1 \, \text{cm}^3$ scintillator bars arranged in two layers to cover both x and y views, called horizontal (H) or vertical (V). The vertical plane (DS V) is instrumented with one SiPM at the top end of each bar, whereas the horizontal plane has two SiPMs, one at each

Figure 4. Top: the seven scintillating bars wrapped in aluminized mylar and aligned side by side. Bottom: PCB hosting the 56 SiPMs.

end (DS R and DS L). To collect cosmic ray data, the DS was placed parallel to the floor, and the Veto 3 plane was positioned horizontally above the DS chamber.
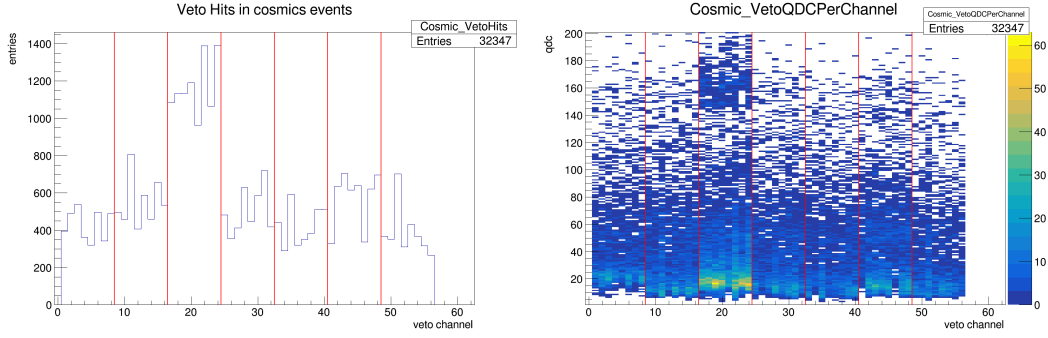
A cosmic ray event was tagged by requiring:

- signals from DS R, L and V. If there was more than one hit, we selected the one with the higher value of integrated charge (QDC - Charge to Digital Conversion), i.e. the larger light input to the SiPMs;

- the signals in DS R and L had to be originated from the same bar;

- all signals to be above a predefined QDC threshold, to further cut noise.

To verify that channels were functional we examined the hit distribution and QDC response. The hit distribution, shown in figure 5 (left), features a peak in the third bar which is not expected for cosmic rays. It was caused by a gain setting that was too high. This is shown in the QDC distribution per channel, figure 5 (right), in which a saturation effect is visible for this bar.
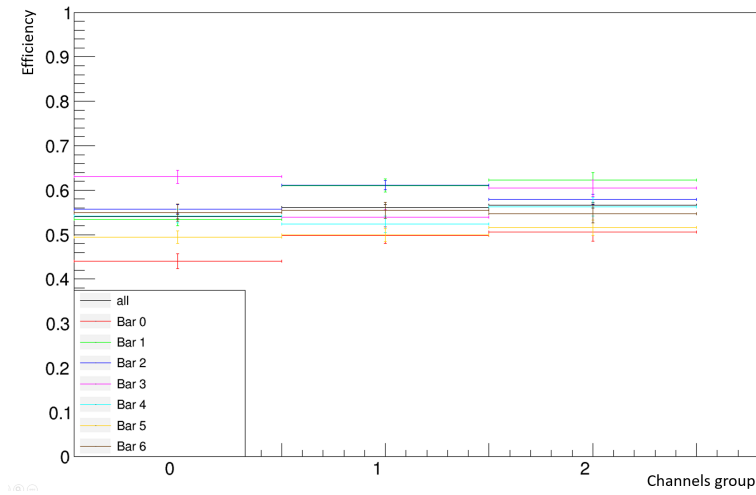
To reduce the contribution of background and noise when computing the efficiency, the bar hit in the Veto must be spatially compatible with the expected cosmic ray position measured using the DS chamber. Moreover, a minimum QDC threshold was set for the veto signal.

To investigate a possible dependence of the efficiency on the position of the hit along the bar caused by the single-sided readout, the hit rate as a function of the hit position was studied. The Veto 3 area was

Figure 5. Hit (left) and QDC (right) distribution per Veto channel in the selected subset of cosmic ray events. The red lines delimit the bars.

divided into 3 bands of 12 cm, measured from the readout side of the bars. To avoid any effect due to the lower efficiency expected at the borders, the first and last three cm were neglected in the computation.

Figure 6. Efficiency Veto 3 bars as a function of the hit position. Each bin is the average of 12 cm. Bin 0 is the side furthest from the readout SiPM. Bin 1 is the central region. The last group is closest to the readout side.

The plot in figure 6 shows the efficiency of each bar as well as the overall detector one as a function of the hit position. As expected, there is a minor and negligible effect due to the distance from the readout. Indeed, the relative efficiency

$$\text{relative efficiency} = \frac{\text{efficiency far from SiPM}}{\text{efficiency close to SiPM}} = 0.95 \pm 0.02$$
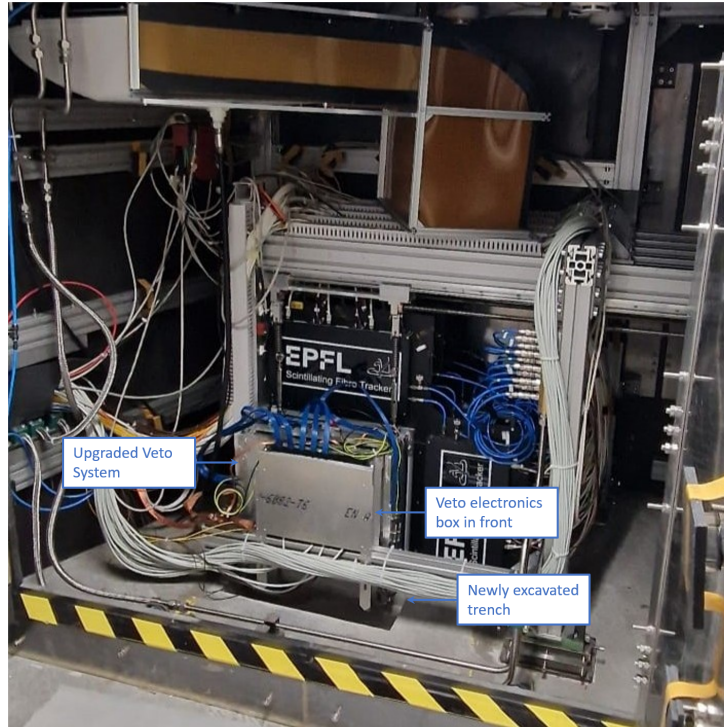
No issues were identified in the cosmic rays test in the laboratory, and the Veto 3 plane was cleared for installation in TI18.

4 Installation and commissioning

With the addition of the third plane, the overall thickness of the Veto system increased, requiring an adjustment of its position in both the upstream and vertical directions; to lower the system sufficiently to cover the target (see figure 3), a trench was cut into the concrete floor.

After completing this civil engineering work, the upgraded Veto system was installed. The final configuration is shown in figure 7, which displays the new trench, the position of the Veto system relative to the rest of the detector, and the box housing its readout electronics.
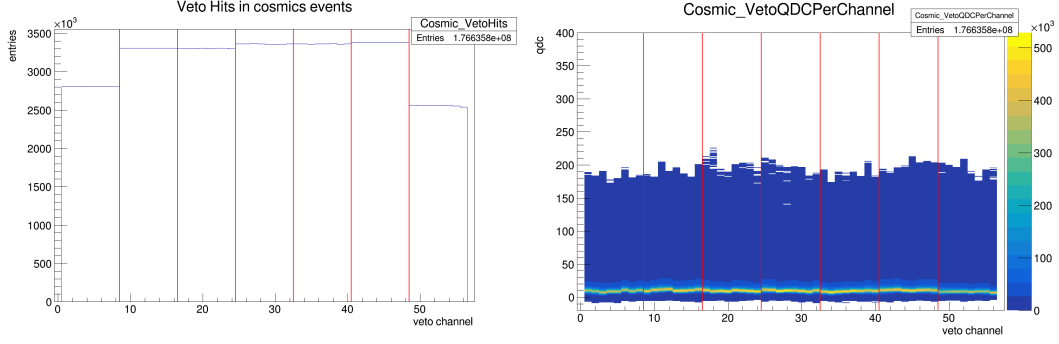

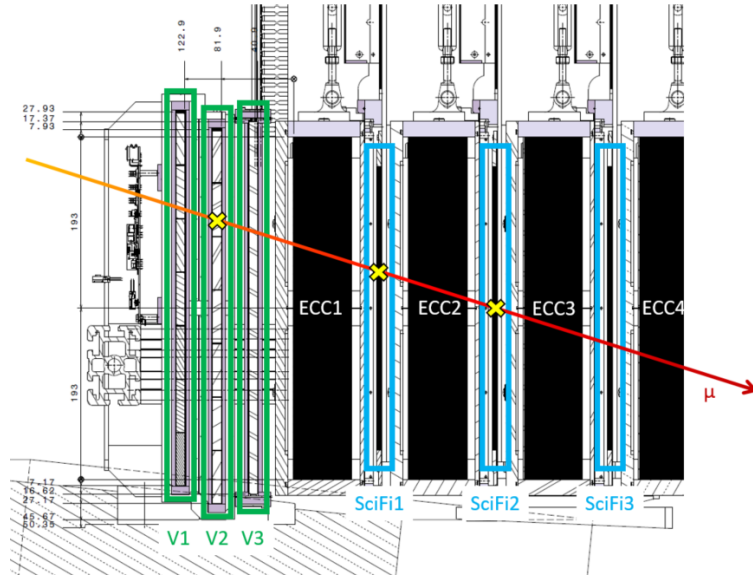**Figure 7.** Final configuration of SND@LHC detector with upgraded Veto system.

The Veto 3 was commissioned using cosmic rays. The hit distribution per channel (see figure 8) shows that the Veto plane was not damaged during transport and installation and that all channels were correctly taking data. The thresholds and gain settings adopted in the TI18 configuration effectively address the issues of electronic noise and QDC saturation that were identified during the laboratory testing phase (see section 3). By carefully calibrating and tuning these parameters in TI18 conditions, the performance limitations encountered in the initial setup were mitigated, resulting in reduced noise and no QDC saturation.

Cosmic ray events were selected by requiring signals in Veto 2 and the first two SciFi modules as shown in figure 9. This allowed the computation of the expected signal position, ensuring that the particle trajectory crossed the Veto plane under study. An additional requirement on the maximum incoming angle of the muon was introduced to avoid a bias in the efficiency calculation. In particular, we required a maximum displacement of $1.5\,\mathrm{cm}$ in the x and y directions between the hits in the two SciFi planes. These requirements are the same for detecting muons from LHC collisions since they traverse the detector horizontally. The Veto plane was considered efficient if there was a hit and the signal was found in the expected bar or the neighbouring ones.

The efficiency distribution is shown in figure 10. It is uniform and close to 1 in all detector areas. The vertical drops correspond to the bar edges as expected, while the lines at $x \simeq 38\,\mathrm{cm}$ and $y \simeq 38\,\mathrm{cm}$ delimit the SciFi acceptance. This also confirms that the single-side readout does not affect the efficiency, as already indicated by the preliminary result given in section 3.

Figure 8. Veto 3 Hit (left) and QDC (right) distribution in cosmic ray events selected in TI18. The red lines delimit the scintillator bars.

Figure 9. Schematic representation of the selection of cosmic ray events. The Veto planes are highlighted in green. The SciFi modules are identified in blue.
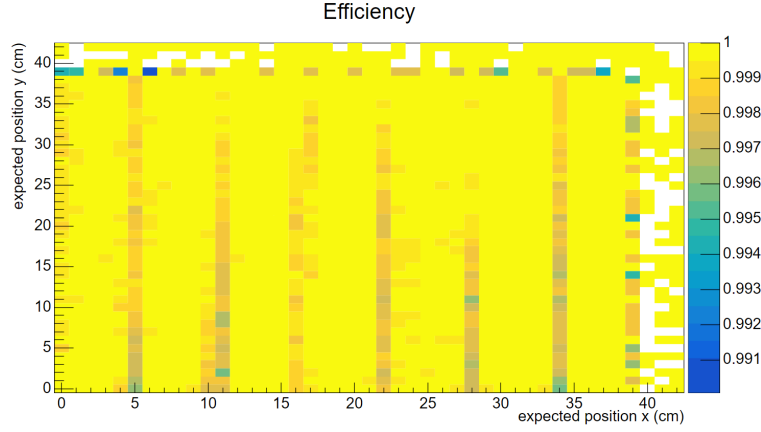
5 Measured Veto inefficiency

The individual Veto plane inefficiencies are estimated using passing through muons by extrapolating reconstructed tracks in the SciFi and the DS to each plane. A plane is considered inefficient if it registers no hit where one is expected because of a passing track (see [6]).

The results shown here are obtained using $102\,\mathrm{fb}^{-1}$ of the delivered luminosity of which 8×10^8 high-quality passing through muon events were selected.

The x-y positions of SciFi tracks for which there is no corresponding Veto plane hit are shown in figure 11. The dead areas in between scintillating bars are visible. As for 2022 and 2023 (see figure 2) there are areas outside the acceptance of a given Veto plane which are densely populated with tracks, especially the horizontal band below Veto 1. However, these regions are enclosed in the sensitive areas of the other planes, as shown in the combined system plot in figure 12. The selected area of best system performance, a fiducial area of $40 \times 48\,\mathrm{cm}^2$ in ranges $-47\,\mathrm{cm} \leq \mathrm{x} \leq -7\,\mathrm{cm}$ and $10\,\mathrm{cm} \leq \mathrm{y} \leq 58\,\mathrm{cm}$, shown as green rectangles in figures 11 and 12 yields an overall Veto system inefficiency of $(4.9 \pm 1.9) \times 10^{-9}$.
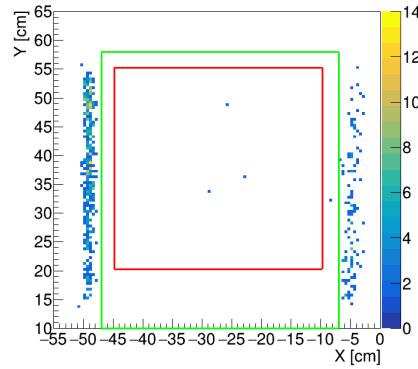
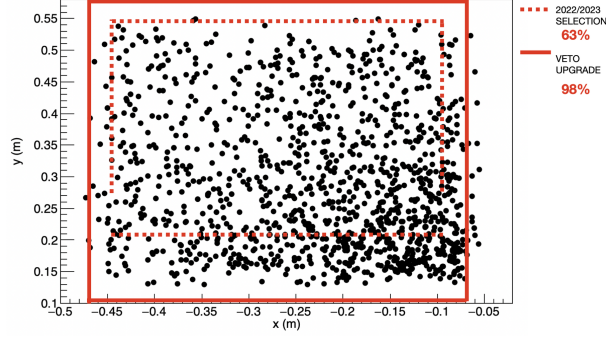**Figure 10.** Veto 3 efficiency measured during commissioning.

Figure 11. The extrapolated position of the reconstructed SciFi tracks at Veto 1 (left) and Veto 2 (middle) and Veto 3 (right) for events without any fired Veto channel in that plane. The red square encloses the fiducial area used for the 2022-2023 analyses; the green rectangle delimits the fiducial area used in 2024.

Figure 12. The extrapolated position of the reconstructed SciFi tracks at Veto 1 for events without any fired Veto channel in all three planes. The red square encloses the fiducial area used for the 2022-2023 analyses, while the green rectangle represents the fiducial area used in the 2024 Veto inefficiency study.

The fiducial area for neutrino interactions is now 1.6 times larger than the area used in the 2022-2023 analysis and fully covers the target region. Monte Carlo simulation studies suggest that this could lead to an increase of 56% of observable neutrino interactions, see figure 13.

Figure 13. Position of muon neutrino interactions from Monte Carlo simulation. The dashed line represents the fiducial area used in 2022-2023, while the solid one encloses the acceptance of the upgraded Veto system.

6   Summary

In this paper, we reported the construction of the Veto 3 and its performance during commissioning, and the relocation of the Veto system in TI18 during the 2023-2024 YETS.

The upgraded Veto system fully covers the target region and allows for extending the fiducial acceptance to neutrino interactions into the whole target volume.

After lowering the Veto system and adding a third Veto module with vertical bars, the optimal inefficiency of the Veto system was reduced from $(7.8 \pm 2.8) \times 10^{-8}$ in 2022-2023 on a fiducial area corresponding to 64% of the target to $(4.9 \pm 1.9) \times 10^{-9}$ in 2024 with full target coverage. Monte Carlo simulation studies suggest that the larger fiducial volume and reduced inefficiency could give an increase of 56% of observable neutrinos.

References

[1] SND@LHC collaboration, *SND@LHC: the scattering and neutrino detector at the LHC*, 2024 *JINST* **19** P05067 [arXiv:2210.02784].

[2] SND@LHC collaboration, *Observation of Collider Muon Neutrinos with the SND@LHC Experiment*, *Phys. Rev. Lett.* **131** (2023) 031802 [arXiv:2305.09383].

[3] SND@LHC collaboration, *Measurement of the muon flux at the SND@LHC experiment*, *Eur. Phys. J. C* **84** (2024) 90 [arXiv:2310.05536].

[4] Hamamatsu, *S14160-6050HS*, https://www.hamamatsu.com/eu/en/product/optical-sensors/mppc/mppc_mppc-array/S14160-6050HS.html.

[5] R. Bugalho et al., *Experimental characterization of the TOFPET2 ASIC*, 2019 *JINST* **14** P03029.

[6] SND@LHC collaboration, *Installation of the 3rd Veto plane*, Tech. Rep. SNDLHC-NOTE-2025-001 (2024).

The SND@LHC collaboration

D. Abbaneo [9], G. Acampora [1,2], S. Ahmad [42], R. Albanese [1,2], A. Alexandrov [1], F. Alicante [1,2], F. Aloschi [1,2], K. Androsov [6], A. Anokhina [3], C. Asawatangtrakuldee [38], M.A. Ayala Torres [32,27], N. Bangaru [1,2], C. Battilana [4,5], A. Bay [6], A. Bertocco [1,2], C. Betancourt [7], D. Bick [8], R. Biswas [9], A. Blanco Castro [10], V. Boccia [1,2], M. Bogomilov [11], D. Bonacorsi [4,5], W.M. Bonivento [12], P. Bordalo [10], A. Boyarsky [13,14], S. Buontempo [1], V. Cafaro [4], M. Campanelli [15], T. Camporesi [10], V. Canale [1,2], D. Centanni [1,16], F. Cerutti [9], V. Chariton [1,2], M. Chernyavskiy [3], A. Chiuchiolo [21], K.-Y. Choi [17], F. Cindolo [4], M. Climescu [18], A. Crupano [4], G.M. Dallavalle [4], N. D'Ambrosio [45], D. Davino [1,20], P.T. de Bryas [6], G. De Lellis [1,2], M. de Magistris [1,16], G. Del Giudice [1,2], G. De Marzi [21], S. De Pasquale [21], A. De Roeck [9], S. De Pasquale [21], A. De Rújula [9], D. De Simone [7], H. De Souza Santos [10], M.A. Diaz Gutierrez [7], A. Di Crescenzo [1,2], C. Di Cristo [1,2], D. Di Ferdinando [4], C. Dinc [23], R. Donà [4,5], O. Durhan [23,43], D. Fasanella [4], O. Fecarotta [1,2], F. Fedotovs [15], M. Ferrillo [7], A. Fiorillo [1,2], R. Fresa [1,2], N. Funicello [21], W. Funk [9], V. Giordano [4], A. Golutvin [26], E. Graverini [6,41], L. Guiducci [4,5], A.M. Guler [23], V. Guliaeva [37], G.J. Haefeli [6], C. Hagner [8], J.C. Helo Herrera [27,40], E. van Herwijnen [26], A. Iaiunese [1,16], P. Iengo [1,2], S. Ilieva [9,11], S.A. Infante Cabanas [40,27], A. Infantino [9], A. Iuliano [1], C. Kamiscioglu [23], A.M. Kauniskangas [6], E. Khalikov [3], S.H. Kim [29], Y.G. Kim [30], G. Klioutchnikov [9], M. Komatsu [31], N. Konovalova [3], S. Kuleshov [27,32], L.Krzempek [1,2,9], H.M. Lacker [19], O. Lantwin [1], F. Lasagni Manghi [4], A. Lauria [1,2], K.Y. Lee [29], K.S. Lee [33], W.-C. Lee [8], V.P. Loschiavo [1,20], A. Margiotta [4,5], A. Mascellani [6], M. Majstorovic [9], F. Mei [4,5], A. Miano [1,44], A. Mikulenko [13], M.C. Montesi [1,2], F.L. Navarria [4,5], W. Nuntiyakul [39], S. Ogawa [34], N. Okateva [3], M. Ovchynnikov [9], G. Paggi [4,5,*], A. Perrotta [4], D. Podgrudkov [3], N. Polukhina [3], F. Primavera [4], A. Prota [1,2], A. Quercia [1,2], S. Ramos [10], A. Reghunath [19], T. Roganova [3], F. Ronchetti [6], T. Rovelli [4,5], O. Ruchayskiy [35], T. Ruf [9], Z. Sadykov [3], M. Samoilov [3], V. Scalera [1,16], W. Schmidt-Parzefall [8], O. Schneider [6], G. Sekhniaidze [1], N. Serra [7], M. Shaposhnikov [6], V. Shevchenko [3], T. Shchedrina [1,2], L. Shchutska [6], H. Shibuya [34,36], G.P. Siroli [4,5], G. Sirri [4], G. Soares [10], J.Y. Sohn [29], O.J. Soto Sandoval [27,40], M. Spurio [4,5], N. Starkov [3], J. Steggemann [6], D. Strekalina [1,2], I. Timiryasov [35], V. Tioukov [1], F. Tramontano [1,2], C. Trippl [6], E. Ursov [19], A. Ustyuzhanin [1,37], G. Vankova-Kirilova [11], G. Vasquez [7], V. Verguilov [11], N. Viegas Guerreiro Leonardo [10], L. A. Viera Lopes [10], C. Vilela [10], C. Visone [1,2], R. Wanke [18], S. Yamamoto [31], Z. Yang [6], C. Yazici [1], S.M. Yoo [17], C.S. Yoon [29], E. Zaffaroni [6], J. Zamora Saa [27,32]

1 *Sezione INFN di Napoli, Napoli, 80126, Italy*
2 *Università di Napoli "Federico II", Napoli, 80126, Italy*
3 *Affiliated with an institute formerly covered by a cooperation agreement with CERN*
4 *Sezione INFN di Bologna, Bologna, 40127, Italy*
5 *Università di Bologna, Bologna, 40127, Italy*
6 *Institute of Physics, EPFL, Lausanne, 1015, Switzerland*
7 *Physik-Institut, UZH, Zürich, 8057, Switzerland*
8 *Hamburg University, Hamburg, 22761, Germany*
9 *European Organization for Nuclear Research (CERN), Geneva, 1211, Switzerland*
10 *Laboratory of Instrumentation and Experimental Particle Physics (LIP), Lisbon, 1649-003, Portugal*
11 *Faculty of Physics,Sofia University, Sofia, 1164, Bulgaria*
12 *Università degli Studi di Cagliari, Cagliari, 09124, Italy*
13 *University of Leiden, Leiden, 2300RA, The Netherlands*
14 *Taras Shevchenko National University of Kyiv, Kyiv, 01033, Ukraine*

[15] *University College London, London, WC1E6BT, United Kingdom*

[16] *Università di Napoli Parthenope, Napoli, 80143, Italy*

[17] *Sungkyunkwan University, Suwon-si, 16419, Korea*

[18] *Institut für Physik and PRISMA Cluster of Excellence, Mainz, 55099, Germany*

[19] *Humboldt-Universität zu Berlin, Berlin, 12489, Germany*

[20] *Università del Sannio, Benevento, 82100, Italy*

[21] *Dipartimento di Fisica 'E.R. Caianello', Salerno, 84084, Italy*

[23] *Middle East Technical University (METU), Ankara, 06800, Turkey*

[26] *Imperial College London, London, SW72AZ, United Kingdom*

[27] *Millennium Institute for Subatomic physics at high energy frontier-SAPHIR, Santiago, 7591538, Chile*

[29] *Department of Physics Education and RINS, Gyeongsang National University, Jinju, 52828, Korea*

[30] *Gwangju National University of Education, Gwangju, 61204, Korea*

[31] *Nagoya University, Nagoya, 464-8602, Japan*

[32] *Center for Theoretical and Experimental Particle Physics, Facultad de Ciencias Exactas, Universidad Andrès Bello, Fernandez Concha 700, Santiago, Chile*

[33] *Korea University, Seoul, 02841, Korea*

[34] *Toho University, Chiba, 274-8510, Japan*

[35] *Niels Bohr Institute, Copenhagen, 2100, Denmark*

[36] *Present address: Faculty of Engineering, Kanagawa, 221-0802, Japan*

[37] *Constructor University, Bremen, 28759, Germany*

[38] *Chulalongkorn University, Bangkok, 10330, Thailand*

[39] *Chiang Mai University , Chiang Mai, 50200, Thailand*

[40] *Departamento de Física, Facultad de Ciencias, Universidad de La Serena, La Serena, 1200, Chile*

[41] *Also at: Università di Pisa, Pisa, 56126, Italy*

[42] *Affiliated with Pakistan Institute of Nuclear Science and Technology (PINSTECH), Nilore, 45650, Islamabad, Pakistan*

[43] *Also at: Atilim University, Ankara, Turkey*

[44] *Affiliated with Pegaso University, Napoli, Italy*

[45] *Affiliated withg Laboratori Nazionali del Gran Sasso, L'Aquila, 67100, Italy*

[*] *Corresponding author*